GPR Relative Localization Method Based on Saliency Detection and Intermittent Fusion

1st Huaichao Wang
Civil Aviation University of China
Tianjin, China
0009-0009-6903-742X

2nd Xinyu Guo
Civil Aviation University of China
Tianjin, China
0009-0009-8172-7095

3rd Xuanxin Fan
Civil Aviation University of China
Tianjin, China
0009-0007-8958-1567

4th Lei Sun
Nankai University
Tianjin, China
0000-0002-8886-9012

5th Haifeng Li*
Civil Aviation University of China
Tianjin, China
0000-0003-0311-8293

6th Kairat Koshekov
Civil Aviation Academy
Almaty, Kazakhstan
0000-0002-9586-2310

7th Dezhen Song
Mohamed Bin Zayed University of Artificial Intelligence (MBZUAI)
Abu Dhabi, UAE
0000-0002-2944-5754

***Abstract*—When performing robot/vehicle localization using Ground Penetrating Radar (GPR) to handle adverse weather and environmental conditions, existing GPR-based relative localization methods are prone to generating unreliable displacement estimates in feature-sparse regions. Direct implementation of continuous fusion propagates errors induced by these erroneous estimates into the entire system, which in turn degrades the trajectory accuracy. This paper proposes a GPR intermittent fusion localization method based on saliency detection and filtering. Specifically, a three-branch HVS-Net saliency detection network is employed to assess the feature saliency of consecutive B-scan image pairs. Only when the image pair features are deemed salient are they introduced as observations into the factor graph-based fusion framework. Experiments on the public CMU-GPR dataset demonstrate that the proposed saliency detection module can effectively filter out feature-sparse image pairs. Moreover, the intermittent fusion strategy proposed significantly enhances system-level localization accuracy. Relative to continuous fusion, the overall Absolute Trajectory Error (ATE) is reduced by 18.04% (0.081 m). The experimental results verify that the proposed method can effectively suppress the propagation of errors from low-quality GPR observations, thereby improving localization stability and accuracy in complex subsurface environments.**

***Index Terms*—Ground Penetrating Radar (GPR), Multi-sensor Fusion, Intermittent Fusion, Factor Graph, Deep Learning.**

I. INTRODUCTION

Precise localization of robots and vehicles in challenging weather and environmental scenarios is essential for autonomous driving. Popular localization methods rely on onboard sensors such as the Global Positioning System (GPS) receiver, cameras, LiDAR, and Inertial Measurement Units (IMU). However, these methods are significantly hampered in environments such as urban canyons, tunnels, or under adverse weather conditions, which presents significant safety challenges for autonomous driving. Compared to the variable surface environment, subsurface structures are typically more stable, which provides a unique advantage for localization using subsurface features. Ground Penetrating Radar (GPR), with its non-destructive penetration and detection capability for subsurface media, makes it a highly promising supplementary sensor in multi-sensor fusion systems. This technology has shown significant value in various engineering fields, such as coal gangue identification for intelligent mining [1], subsurface defect detection in airport runways, and the investigation of subsurface structures on celestial bodies like Mars in planetary exploration [2]–[4]. It is also widely used in geological surveys and pipeline detection, highlighting its adaptability and potential. Given this capability, subsurface feature-based detection is now being applied to the field of localization. To overcome the inherent limitations of any single sensor,

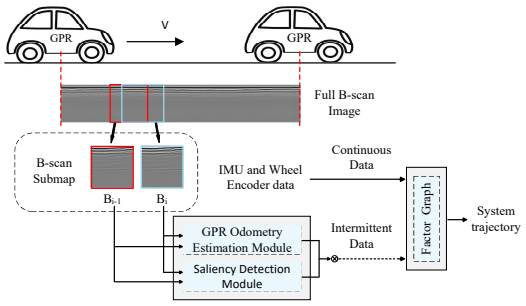

Fig. 1: System Architecture Overview

This work was supported in part by National Science Foundation of China under grant 62373365, by the Fundamental Research Funds for the Central Universities under grant 3122024PT08, 3122025089, and by the Tianjin "Belt and Road" Joint Research Program under Grant 24PTLYHZ00230.

*Corresponding Email: hfli@cauc.edu.cn.

multi-sensor fusion methods have been widely adopted. These systems integrate data from different sensors, enabling them to maintain stable performance by relying on other sensors when one temporarily fails, thus enhancing overall localization robustness and accuracy [5].

This paper investigates multi-sensor fusion localization methods based on GPR. To address the issue of large errors in feature-sparse regions produced by current GPR-based relative localization methods, we introduce a custom-designed, three-branch HVS-Net saliency detection model to assess whether consecutive B-scan image pairs are suitable for displacement estimation. A factor graph, triggered for optimization based on accumulated IMU data and fixed time intervals, is employed to achieve intermittent fusion of GPR odometry estimates with other sensors. This prevents unreliable GPR odometry estimates from causing errors in the multi-sensor fusion system. The main contributions of this paper are summarized as follows:

- A GPR intermittent fusion localization framework based on saliency detection is proposed. This framework employs a purpose-designed HVS-Net to assess the quality of B-scan image pairs, and only fuses reliable observations selectively, thereby suppressing error propagation at the source.
- A novel three-branch HVS-Net is designed for the saliency detection of GPR B-scan images, where the three branches are dedicated to horizontal, vertical, and standard feature extraction, respectively. This specialized structure enhances the model's ability to capture discriminative features of B-scan images.
- The factor graph optimization strategy is improved by triggering updates based on both accumulated IMU data and fixed time intervals. This approach avoids interpolation during long-term absence of GPR data, enabling adaptive and high-precision multi-sensor fusion.

II. RELATED WORK

Currently, GPR-based localization methods are generally divided into two categories: absolute and relative localization. Absolute localization typically involves two scans: one to create a map library of subsurface features, and another to match current GPR data with the map for global positioning. MIT's LGPR system demonstrated its feasibility under complex weather conditions such as rain and snow [6]–[8]. To improve matching robustness, Zhang et al. proposed a multi-sequence matching strategy using a U-Net network to extract common features [9]. Rule-based methods, such as the Dominant Energy Curve (DEC) [10] and CDSC descriptors [11], have also been explored. With the development of deep learning, Zhang et al. introduced EDE-Net for automatic feature extraction and map matching [12]. Ni Zhikang et al. improved robustness through a two-stage strategy combining global coarse localization and local refinement [13]. Bi et al. addressed feature sparsity using 3D multi-channel GPR data for direct coordinate estimation via TSVR-Net [14]. However, these methods depend on pre-constructed maps and require re-acquisition when subsurface structures change.

Relative localization methods focus on recursively estimating the system's motion state over time. The core idea is to estimate relative displacement between adjacent keyframes by analyzing consecutive B-scan images with sufficient overlap, and then construct the trajectory through incremental accumulation of these displacements. Baikovitz et al. proposed a method based on a learned sensor model, using ResNet18 to extract features and Pearson correlation to measure similarity, followed by a fully connected network for displacement regression [15]. Building on this, Van et al. incorporated a type-2 fuzzy inference system to improve estimation accuracy [16]. Wickramanayake et al. adopted an end-to-end CNN-LSTM architecture to regress displacement from multiple consecutive image pairs [17]. However, existing methods often do not adequately address challenging conditions such as sparse subsurface features or unstable platform motion.

To address the above issues, this paper proposes a strategy combining a saliency detection network and an intermittent fusion mechanism. The saliency network evaluates whether consecutive B-scan image pairs contain sufficient features for reliable estimation. Only valid odometry results are incorporated into the factor graph, while unreliable data is excluded. This mechanism enables intermittent fusion with other sensors, improving localization accuracy and robustness in complex environments.

III. METHODOLOGY

A. System Architecture Overview

This paper proposes an improved scheme based on saliency detection and intermittent fusion. The overall system architecture is illustrated in Fig. 2. A three-branch HVS-Net acts as a gating module to assess if consecutive B-scan image pairs have sufficient salient features, determining whether GPR odometry estimates are included in fusion. The GPR odometry module only provides displacement estimates from validated pairs for fusion. Under the factor graph framework, optimization is triggered by accumulated IMU data or fixed intervals, avoiding forced interpolation during GPR data loss and realizing adaptive intermittent fusion of GPR, wheel encoder and IMU observations to generate trajectories.

B. Data Preprocessing

Data preprocessing follows the method of the public CMU-GPR dataset and results in Fig. 3. First, raw complete trajectory GPR data is processed into B-scan images, which are then segmented into overlapping sub-images organized into image pairs as system input. Key steps include: Dewow Filter (polynomial fitting to remove low-frequency DC components and baseline drift), Butterworth Filter (suppressing high-frequency noise and low-frequency drift), FIR Bandpass Filter (200-850 MHz passband, 5 GHz sampling frequency), SEC gain (compensating signal attenuation), Wavelet Denoising (discrete wavelet transform for noise suppression), and 1D Horizontal Gaussian Smoothing (improving image SNR

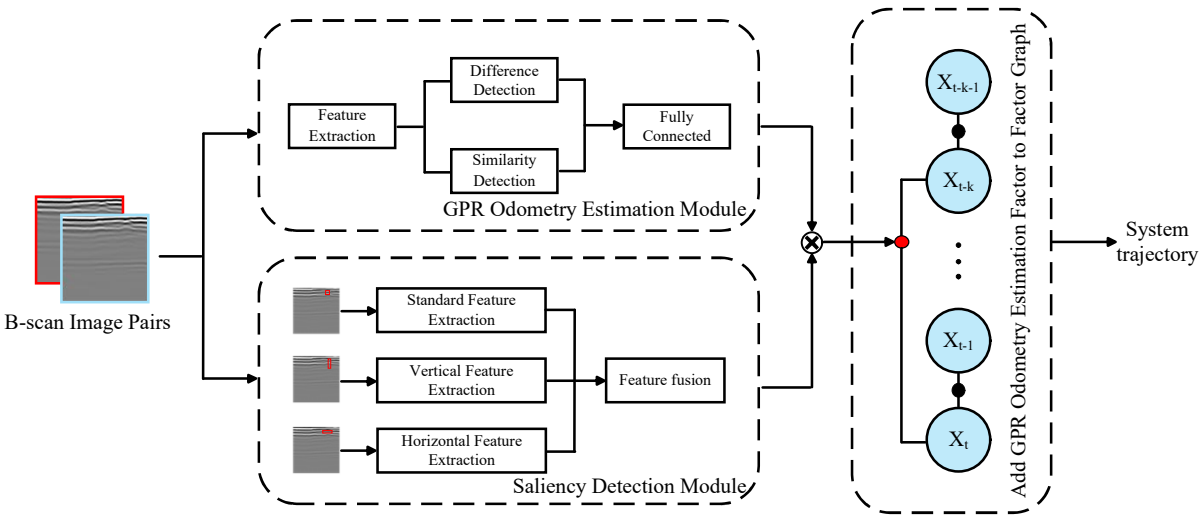

Fig. 2: System Architecture for Multi-sensor Fusion Localization

while preserving edges). Preprocessed A-scan data becomes overlapping B-scan image pairs for subsequent modules. The saliency detection and GPR odometry estimation modules use independent parameters but share the same image pairs.

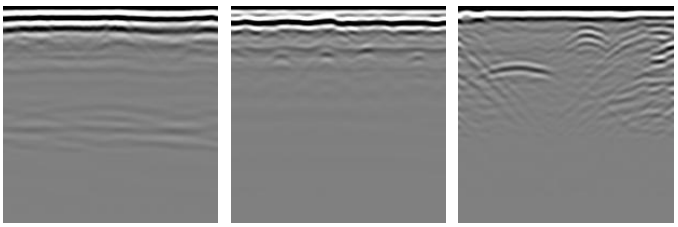

(a) gates_g (b) nsh_b (c) nsh_h

Fig. 3: Preprocessed B-scan images under various scenarios

C. Saliency Detection Module

In B-scan images acquired by GPR, reflections from subsurface targets often present as hyperbolic features with distinct directionality. Simultaneously, structures such as bedding planes and material inhomogeneities contribute abundant texture information. To support saliency detection on B-scan image pairs, we designed a three-branch convolutional neural network termed HVS-Net. The network architecture is shown in Fig. 4. It contains three independent feature extraction paths: Horizontal, Vertical, and Standard, designed to capture structural information and texture patterns in different orientations within the B-scan image. This design is primarily motivated by the imaging characteristics inherent to B-scan GPR data. In the horizontal branch, convolution operations are used to extract features along the horizontal direction, helping to capture continuous features along the scanning direction and horizontal bedding. The formula is as follows:

$$F_{\text{horiz}} = \text{Conv2d}(I_{\text{input}}, W_{\text{horiz}}, S) \tag{1}$$

where F_{horiz} is the feature map extracted by the horizontal branch, I_{input} is the input image, W_{horiz} is the kernel used for the horizontal convolution, and S is the stride of the convolution operation. Similarly, the vertical branch uses convolution operations to extract reflection features along the vertical direction, enhancing the ability to capture vertical reflection features. The formula is as follows:

$$F_{\text{vert}} = \text{Conv2d}(I_{\text{input}}, W_{\text{vert}}, S) \tag{2}$$

where F_{vert} is the feature map extracted by the vertical branch, W_{vert} is the kernel used for the vertical convolution. For general local feature extraction, the standard branch uses convolution operations to capture typical texture information within the image.

$$F_{\text{std}} = \text{Conv2d}(I_{\text{input}}, W_{\text{std}}, S) \tag{3}$$

where F_{std} is the feature map extracted by the standard branch, W_{std} is the kernel used for the standard convolution. After extracting features from the three branches, their outputs are concatenated along the channel dimension to form a combined feature map for further processing.

$$F_{\text{concat}} = \text{Concat}(F_{\text{horiz}}, F_{\text{vert}}, F_{\text{std}}) \tag{4}$$

The concatenated feature map F_{concat} is then passed through a feature fusion module, which uses convolution operations to integrate the information and extract the final feature representation. The formula for this fusion operation is as follows:

$$F_{\text{fusion}} = \text{Conv2d}(F_{\text{concat}}, W_{\text{fusion}}, S) \tag{5}$$

where F_{fusion} is the fused feature map, W_{fusion} is the kernel used for the final convolution in the fusion module, and S is the stride of the convolution operation. By fusing features from

these three branches, the network can more comprehensively extract the content of B-scan images, thereby enhancing its ability to determine whether an image pair contains sufficiently discriminative features.

The function of this saliency detection module is to perform binary saliency detection on the input consecutive B-scan image pairs, determining whether they contain sufficient features to support reliable displacement estimation. If an image pair is identified as having salient features, it is sent to the subsequent GPR odometry module for relative displacement calculation, and the estimated result is passed to the factor graph for multi-sensor fusion optimization. Conversely, if an image pair is identified as feature-sparse or of poor quality, the system skips displacement estimation and fusion for that pair and proceeds to the next data instance. This selective processing mechanism can effectively filter out low-information image pairs caused by excessive noise or weak features, preventing them from introducing significant errors during the odometry estimation stage. This enhances the robustness of the multi-sensor fusion system and improves overall localization accuracy.

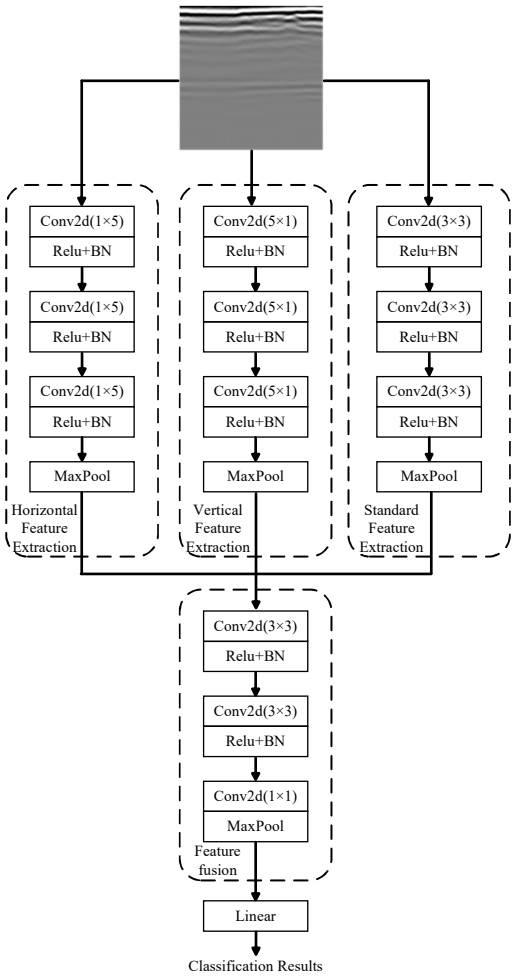

Fig. 4: Architecture of the HVS Network

D. GPR Odometry Estimation

The core task of the GPR odometry estimation module is to regress the one-dimensional relative displacement of the sensor platform inferred from consecutively acquired B-scan image pairs. The underlying principle is that, during continuous radar scanning along a motion trajectory, adjacent B-scan images exhibit significant data overlap and feature correlation. By quantifying feature variations or signal correlations between two image frames, the sensor motion increment over the corresponding time interval can be indirectly inferred.

GPR-OdomNet [19] is a neural network architecture designed to estimate the relative displacement between consecutive B-scan image pairs. The simplified structure of GPR-OdomNet is shown in Fig. 5. It employs two parallel pathways to capture both dissimilarity and similarity information, which are fused to regress the displacement value. The dissimilarity path computes the absolute difference between feature maps and employs attention mechanisms to emphasize motion-relevant patterns. The similarity path evaluates inter-frame consistency via cosine similarity of high-level feature representations. The pooled features from both pathways are then concatenated and passed to a fully connected regression module. The network is trained end-to-end using total station measurements as supervision, with an RMSE loss function. This complementary learning of dissimilarity and similarity significantly improves the robustness and accuracy of GPR-based displacement estimation.

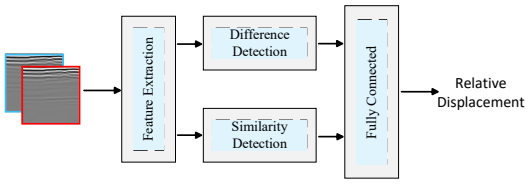

Fig. 5: Architecture of the OdomNet

E. Factor Graph Fusion

In the multi-sensor fusion stage, a factor graph model is employed to fuse observations from the GPR odometry, wheel encoder, and IMU for estimating the system motion trajectory. In the factor graph, system state variables (including position, velocity, attitude, and other kinematic states) are modeled as nodes, while observations from each sensor are formulated as constraint edges connecting the corresponding nodes.

In conventional factor graph optimization frameworks, higher-frequency sensor measurements are typically interpolated to align with lower-frequency timestamps, and updates from the lower-frequency sensor are used to trigger optimization. To ensure uniform temporal sampling within the factor graph, GPR measurements would conventionally require interpolation. However, considering that GPR data may have prolonged missing segments after filtering, interpolation is not performed over these long gaps introduced by the filtering

process. In addition, to preserve the accuracy of wheel encoder measurements, interpolation is also avoided.

Based on the above considerations, to enable intermittent fusion of one-dimensional GPR odometry with other sensor data, the factor graph optimization trigger condition is defined as follows: optimization is executed only when IMU data accumulates to a certain amount or when a fixed time interval is reached. As shown in Fig. 6, each keyframe contains four state nodes, while the WE and GPR constraint edges are incorporated into the factor graph as constraints only when corresponding observation data exists between adjacent keyframes. This method avoids interpolating GPR data over long intervals resulting from filtering, thereby reducing the errors introduced by such interpolation.

The constructed factor graph structure is shown in Fig. 6. Each keyframe contains four nodes representing the 6-degree-of-freedom pose (3D rotation R_t and 3D translation P_t), 3D velocity v_t, 3D gyroscope bias $b_{g,t}$, and 3D accelerometer bias $b_{a,t}$, which together form the 15-dimensional system state vector. The graph includes five types of constraint edges: the IMU pre-integration edge constrains poses, velocities, and biases between adjacent keyframes; the BI edge models the random-walk behavior of gyroscope and accelerometer biases, imposing constraints between bias nodes at consecutive time steps; the WE edge and GPR edge impose velocity constraints derived from odometry estimates of the wheel encoder and GPR, where the odometry estimates are first obtained and then converted into velocity observations according to their timestamps, respectively; the current keyframe node is constrained by the previous keyframe node.

With the above factor graph model, the multi-sensor fusion problem is transformed into a Maximum a Posteriori (MAP) estimation problem over the node states. The Levenberg–Marquardt (LM) nonlinear optimization algorithm is then employed to solve this problem, yielding the optimal estimate of the system trajectory. This factor graph framework can effectively fuse sensor observation data with different frequencies and characteristics. Moreover, when one sensor temporarily fails or observation quality degrades, the system can still rely on the remaining sensors to maintain localization performance, demonstrating strong robustness and adaptability to varying environments.

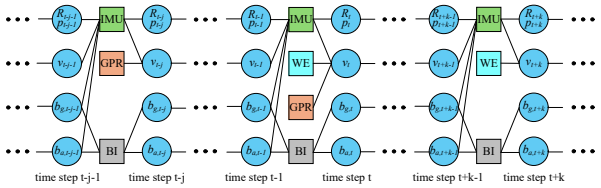

Fig. 6: Factor Graph Model

IV. EXPERIMENT AND EVALUATION

To evaluate the effectiveness of the proposed method, experiments are conducted on a public dataset. First, the dataset is introduced. Then, a quantitative analysis of the saliency detection module and its contribution to the multi-sensor fusion system is performed. Finally, the overall experimental results are summarized.

A. Dataset Introduction

The experiments use the publicly released CMU-GPR dataset [18] from Carnegie Mellon University (CMU). It synchronously provides wheel encoder, GPR, IMU, and high-precision total station data. In this work, IMU, wheel encoder, and GPR measurements are used as inputs, while the total station trajectory serves as ground truth. The dataset contains three scenarios: a parking garage (gates_g), a basement (nsh_b), and a factory floor (nsh_h). Complete trajectories from each scenario are used for training and testing to evaluate generalization across different subsurface environments.

During training and testing of the saliency detection module, each trajectory is divided into multiple B-scan sub-images and manually labeled as salient-feature or feature-sparse based on prior knowledge. The former contains clear reflection structures suitable for displacement estimation, while the latter includes weak or ambiguous reflections that often lead to unreliable estimates.

Preprocessed B-scan examples are shown in Fig. 3. Significant differences can be observed across scenarios: the parking garage contains sparse and weak reflections, while the factory floor exhibits richer and more distinct structural features.

B. Ablation Study

To evaluate the impact of the saliency detection module on GPR odometry accuracy, the GPR relative displacement estimation model OdomNet is used as the baseline. Performance is compared before and after incorporating the module, as well as across different network variants. RMSE is adopted as the evaluation metric.

$$\text{RMSE} = \sqrt{\frac{1}{n}\sum_{i=1}^{n}(\hat{y}_i - y_i)^2} \tag{6}$$

where n is the total number of samples, y_i is the true value of the i-th displacement, and $\hat{y}_i$ is the corresponding predicted value. A smaller RMSE indicates a smaller discrepancy between the predicted and true displacements.

Experimental results for OdomNet and its variants are shown in Table I. In this comparison, OdomNet denotes the original network, HVS-OdomNet denotes the complete network after adding the saliency detection module, HV-OdomNet denotes a variant without the standard convolution branch, HS-OdomNet denotes a variant without the vertical feature extraction branch, and VS-OdomNet denotes a variant without the horizontal feature extraction branch. All models share the same pre-trained weights without additional retraining. Results show that HVS-OdomNet reduces the average RMSE by 0.209 cm (7.82%) compared to OdomNet and achieves the best overall performance.

Compared with the full three-branch structure, dual-branch variants generally perform worse and may even underperform

TABLE I: RMSE of Displacement Estimation for Different OdomNet Variants (Unit: cm)

Model	gates_g	nsh_b	nsh_h	All Scenarios
OdomNet	3.894	2.136	1.982	2.671
HV-OdomNet	3.551	2.284	1.945	2.593
HS-OdomNet	3.721	2.287	1.961	2.656
VS-OdomNet	3.774	2.322	1.951	2.682
HVS-OdomNet	3.504	2.048	1.834	**2.462**

TABLE II: RMSE of Absolute Trajectory Error (ATE) for the Different Model (Unit: m)

Model	gates_g	nsh_b	nsh_h	All Scenarios
Learned GPR Method	1.228	0.332	0.251	0.590
SFM	0.468	0.734	0.439	0.568
DEC	0.47	0.52	0.57	0.50
IMU&Wheel Encoder	0.588	1.074	1.015	0.743
OdomNet	0.353	0.751	0.380	0.449
HVS-OdomNet	0.287	0.564	0.458	**0.368**

the original model in some scenarios. This indicates that embedding the three-branch saliency detection module into the one-dimensional GPR odometry estimation network can effectively enhance estimation robustness and accuracy across different scenarios, with each branch contributing positively to the final performance.

Although filtering changes the number of samples, error reduction occurs only when removed samples have larger-than-average errors. This observation indicates that a portion of the prediction errors in the original GPR odometry originates from B-scan image pairs with sparse subsurface features. By filtering such low-quality inputs, the saliency detection module improves the reliability of displacement estimation and consistently enhances performance across scenarios.

C. Multi-Sensor Fusion Localization

To evaluate the proposed intermittent fusion mechanism, comparative experiments are conducted within a factor graph framework. Baselines include IMU–wheel encoder fusion and continuous fusion methods using OdomNet and other GPR odometry models. The RMSE of the ATE, considering trajectory length, is used as the evaluation metric for system localization accuracy, defined as:

$$\text{Weighted-ATE} = \frac{\sum_{i=1}^{M} W_i \cdot \text{ATE}_i}{\sum_{i=1}^{M} W_i} \tag{7}$$

where M is the total number of trajectories, W_i is the length of the i-th trajectory, and ATE_i is the ATE of the i-th trajectory.

The ATE for the i-th trajectory is calculated using the following formula:

$$\text{ATE}_i = \sqrt{\frac{1}{N}\sum_{j=1}^{N} \left\| \text{trans}(\mathbf{P}_j) - \text{trans}(\mathbf{Q}_j) \right\|^2} \tag{8}$$

where N is the total number of poses in the trajectory, j is the position index, $\mathbf{P}_j$ is the system's estimated pose at the j-th moment, and $\mathbf{Q}_j$ is the corresponding ground-truth pose. A lower error value indicates a smaller overall deviation between the estimated trajectory and the true trajectory.

Table II presents the ATE results obtained by different methods. The Learned GPR Method refers to the CMU learning-based model [15], SFM uses the Subsurface Feature Matrix method [20], and DEC is a map-based localization method using Dominant Energy Curve features [10]. IMU&Wheel Encoder represents the results of IMU and wheel encoder fusion localization, which serves as the baseline for comparison. OdomNet, a network based on similarity and dissimilarity detection, is used for continuous fusion comparison [19]. HVS-OdomNet is the proposed localization method that incorporates the saliency detection network HVS-Net to implement intermittent fusion.

The experimental results demonstrate that HVS-OdomNet, which incorporates a saliency detection network and an intermittent fusion strategy, outperforms all other methods. The ATE is reduced in the first two scenarios. In the gates_g scenario, as shown in Fig. 3a, sparse subsurface reflections lead to the largest odometry estimation error due to limited structural features. In the nsh_b scenario (Fig. 3b), dense reinforcing bars generate cyclic reflection patterns, increasing estimation difficulty. Filtering feature-sparse B-scan pairs in these scenarios significantly reduces trajectory error. In contrast, the nsh_h scenario (Fig. 3c) contains clearer and more distinct reflections, resulting in the lowest estimation error. A slight increase in error is observed after filtering, likely because the original estimation is already highly accurate and the trajectory is jointly influenced by IMU and wheel encoder measurements. Some excluded samples may still provide useful information for fusion. Overall, compared to continuous fusion, the proposed intermittent fusion framework reduces the ATE by 0.081 m (18.04%).

Fig. 7 shows the system trajectory under intermittent fusion, and Fig. 8 present the corresponding ATE curves. The results indicate that, after introducing the saliency detection module and intermittent fusion strategy, the performance is generally superior to IMU&Wheel Encoder and continuous fusion. The intermittent fusion strategy introduces GPR observations only when they are reliable, effectively suppressing error propagation. The HVS-Net module identifies feature-sparse inputs that degrade odometry estimation and provides a reliable filtering mechanism. Integrated into the factor graph framework, this approach avoids errors from low-quality observations and improves localization accuracy and robustness across scenarios, demonstrating the effectiveness of the proposed method in complex subsurface environments.

V. CONCLUSION

This paper proposes a GPR intermittent fusion method within a multi-sensor fusion framework. The method introduces GPR as a supplementary sensor and employs a saliency detection module to filter one-dimensional odometry estimates, enabling intermittent fusion with other sensors. To validate

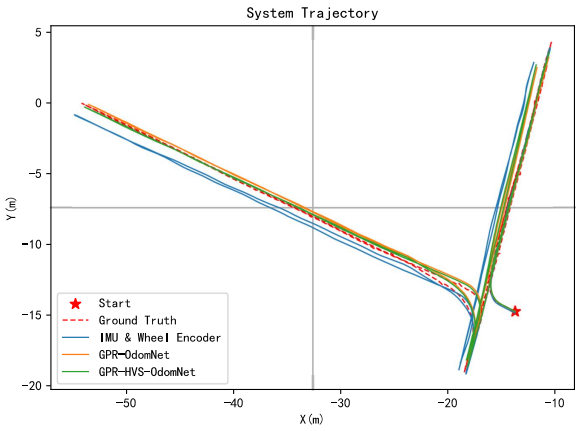

Fig. 7: System Motion Trajectory under Intermittent Fusion with OdomNet Odometry Estimation

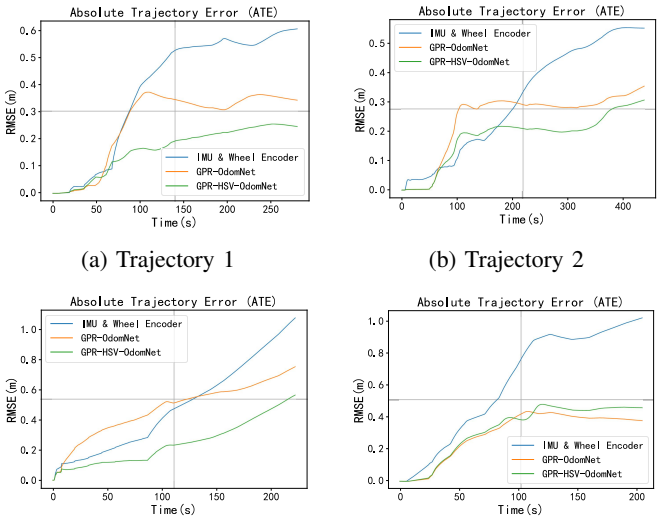

(a) Trajectory 1 (b) Trajectory 2

(c) Trajectory 3 (d) Trajectory 4

Fig. 8: Absolute Trajectory Error (ATE) over time for OdomNet on different trajectories.

the method, comparative and multi-sensor fusion experiments were conducted on the public CMU-GPR dataset. Results show that the intermittent fusion strategy significantly reduces the ATE of GPR odometry methods compared to continuous fusion. Future work will further explore multi-channel GPR-based relative positioning, aiming to achieve independent localization using only multi-channel GPR data.

Acknowledgment

We gratefully acknowledge the authors of the CMU-GPR Dataset for making this publicly available dataset and associated tools accessible, which significantly supported our research.

References

[1] Hao W, Jiang H, Song Q, et al. A multi modal fusion coal gangue recognition method based on IBWO-CNN-LSTM[J]. Scientific Reports, 2024, 14(1): 30396.

[2] Stoker C R, Clarke J, Direito S O L, et al. Mineralogical, chemical, organic and microbial properties of subsurface soil cores from Mars Desert Research Station (Utah, USA): phyllosilicate and sulfate analogues to Mars mission landing sites[J]. International Journal of Astrobiology, 2011, 10(3): 269-289.

[3] Hamran S E, Paige D A, Amundsen H E F, et al. Radar imager for Mars' subsurface experiment—RIMFAX[J]. Space Science Reviews, 2020, 216(8): 128.

[4] Nash J, Dwight Q, Saldyt L, et al. Censible: A robust and practical global localization framework for planetary surface missions[C]//2024 IEEE International Conference on Robotics and Automation (ICRA). IEEE, 2024: 8642-8648.

[5] Bhat S, Kavasseri A. Multi-source data integration for navigation in gps-denied autonomous driving environments[J]. International Journal of Electrical and Electronics Research, 2024, 12(3): 863-869.

[6] Stanley B, Cornick M, Koechling J. Ground penetrating radar based localization[C]//Ground Vehicle Systems Engineering and Technology Symposium, Troy, MI. 2013.

[7] Cornick M, Koechling J, Stanley B, et al. Localizing ground penetrating radar: A step toward robust autonomous ground vehicle localization[J]. Journal of field robotics, 2016, 33(1): 82-102.

[8] Ort T, Gilitschenski I, Rus D. Autonomous navigation in inclement weather based on a localizing ground penetrating radar[J]. IEEE Robotics and Automation Letters, 2020, 5(2): 3267-3274.

[9] Zhang P, Zhi S, Yuan Y, et al. Looking beneath more: A sequence-based localizing ground penetrating radar framework[C]//2024 IEEE International Conference on Robotics and Automation (ICRA). IEEE, 2024: 8515-8521.

[10] Li H, Guo J, Song D. Subsurface feature-based ground robot/vehicle localization using a ground penetrating radar[C]//2024 IEEE International Conference on Robotics and Automation (ICRA). IEEE, 2024: 1716-1722.

[11] Xu J, Lai Q, Wei D, et al. The Ground-Penetrating Radar Image Matching Method Based on Central Dense Structure Context Features[J]. Remote Sensing, 2024, 16(22): 4291.

[12] Zhang P, Chen X, Chen Y, et al. EDENet: Echo Direction Encoding Network for Place Recognition Based on Ground Penetrating Radar[C]//Proceedings of the AAAI Conference on Artificial Intelligence. 2025, 39(10): 10067-10075.

[13] NI Z, YE S, SHI C, et al. A deep learning assisted ground penetrating radar localization method[J]. Journal of electronics and information, 2022, 44(4): 1265-1273.

[14] Bi B, Shen L, Zhang P, et al. TSVR-net: An end-to-end ground-penetrating radar images registration and location network[J]. Remote Sensing, 2023, 15(13): 3428.

[15] Baikovitz A, Sodhi P, Dille M, et al. Ground encoding: Learned factor graph-based models for localizing ground penetrating radar[C]//2021 IEEE/RSJ International Conference on Intelligent Robots and Systems (IROS). IEEE, 2021: 5476-5483.

[16] Van Nam D, Gon-Woo K. Learning type-2 fuzzy logic for factor graph based-robust pose estimation with multi-sensor fusion[J]. IEEE Transactions on Intelligent Transportation Systems, 2023, 24(4): 3809-3821.

[17] Wickramanayake S, Thiyagarajan K, Kodagoda S. Deep learned ground penetrating radar subsurface features for robot localization[C]//2022 IEEE sensors. IEEE, 2022: 1-4.

[18] Baikovitz A, Sodhi P, Dille M, et al. Cmu-gpr dataset: Ground penetrating radar dataset for robot localization and mapping[J]. arXiv preprint arXiv:2107.07606, 2021.

[19] WANG Huaichao, FAN Xuanxin, LIU Ji, et al. GPR-OdomNet: Difference and Similarity-Driven Odometry Estimation Network for Ground Penetrating Radar-Based Localization [J]. arXiv preprint arXiv:2511.17457, 2025.

[20] Li H, Guo J, Fan X, et al. Ground Penetrating Radar-Assisted Multimodal Robot Odometry Using Subsurface Feature Matrix[C]//2025 IEEE 37th International Conference on Tools with Artificial Intelligence (ICTAI). IEEE, 2025: 1030-1036.